Table 1 Patients' demographics (n=42)

Age (years)		Mean±SD 62.0±10.7 Range 35-79
Sex male:female (women: %)		16:26 (62%)
Number of aneurysms		1.3±0.55 Range 1-3
Size of aneurysms		Median 4mm Range 1.5-25
Aneurysm locations		
Anterior cerebral aretry	3	
Acom artery	5	
Middle cerebral artery	20	
Internal carotid artery	13	
IC-pcom artery	5	
Vertebral artery	3	
Basilar artery	5	
Total	54	
Diagnostic modality for aneurysms		
MRA 81.0%, 3D-CTA 69.0%, DSA 14.3% (multiple modalities in 86.0%)		
Duration between diagnosis and interview		
<1 month	5	
1≤ <6 months	17	
6≤ <12 months	7	
12< months	13	
Previous subarachnoid hemorrhage		2/42 (4.8%)
Family history		4/42 (9.5%)

Table 2 Agreement between patients and neurosurgeons on specific treatment and comprehension of treatment options for 6 and 2 categorized scales

Survey question	κ score(95% confidence)	
	6 categorized scales	2 categorized scales
Open surgery is the best treatment for my aneurysm	0.20 (0.02-0.37)	0.62 (0.38-0.86)
Endovascular coiling is the best treatment for my aneurysm	0.28 (0.08-0.48)	0.44 (0.17-0.71)
Leaving it alone is the best treatment for my aneurysm	0.17 (0.02-0.32)	0.67 (0.45-0.89)
Using MRI, CT or angiogram to watch my aneurysm is the best treatment for my aneurysm	0.31 (0.12-0.50)	0.57 (0.33-0.81)
By the end of my appointment today, I understand the treatment options for my aneurysm	0.12 (-0.12-0.37)	NA
By the end of my appointment today, I knew what the best treatment is for my aneurysm	0.01 (-0.20-0.22)	-0.03 (-0.08-0.01)

Table 3 Agreement between patients and experienced (Exp, n=4, 25 pairs) /non-experienced (Non-exp, n=5, 17 pairs) neurosurgeons on specific treatment and comprehension of treatment options for 6 categorized scales

Survey question	κ score(95% confidence)	
	Exp	Non-exp
Open surgery is the best treatment for my aneurysm	0.33(0.10-0.56)	0.00(-0.21-0.22)
Endovascular coiling is the best treatment for my aneurysm	0.21(-0.08-0.51)	0.09(-0.16-0.34)
Leaving it alone is the best treatment for my aneurysm	0.18(-0.05-0.40)	0.15(-0.12-0.41)
Using MRI, CT or angiogram to watch my aneurysm is the best treatment for my aneurysm	0.34(0.10-0.59)	0.25(-0.07-0.58)
By the end of my appointment today, I understand the treatment options for my aneurysm	0.24(-0.07-0.55)	-0.03(-0.44-0.38)
By the end of my appointment today, I knew what the best treatment is for my aneurysm	0.12(-0.15-0.41)	-0.17(-0.52-0.19)

Toshikazu Kimura, M.D.
Department of Neurosurgery, Kanto Medical Center, NTT EC, Tokyo, Japan

Akio Morita, M.D., Ph.D.
Department of Neurosurgery, Kanto Medical Center, NTT EC, Tokyo, Japan

Kengo Nishimura, M.D.
Department of Neurosurgery, Kanto Medical Center, NTT EC, Tokyo, Japan

Hitoshi Aiyama, M.D.
Department of Neurosurgery, Kanto Medical Center, NTT EC, Tokyo, Japan

Hirotaka Itoh, M.D.
Department of Neurosurgery, Kanto Medical Center, NTT EC, Tokyo, Japan

Syunsuke Fukaya, M.D.
Department of Neurosurgery, Kanto Medical Center, NTT EC, Tokyo, Japan

Shigeo Sora, M.D.
Department of Neurosurgery, Kanto Medical Center, NTT EC, Tokyo, Japan

Chikayuki Ochiai, M.D., Ph.D.
Department of Neurosurgery, Kanto Medical Center, NTT EC, Tokyo, Japan

Reprint requests:
Akio Morita, M.D., Ph.D., Department of Neurosurgery, Kanto Medical Center, NTT EC, 5-9-22 Higashigotannda, Shinagawa-ku, Tokyo, Japan 141-8625.
Email: amor-tky@umin.ac.jp

Received, December 26, 2008.
Accepted, May 18, 2009.

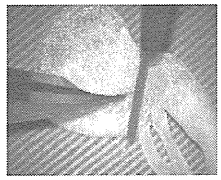

ONLINE DIGITAL VIDEO

SIMULATION OF AND TRAINING FOR CEREBRAL ANEURYSM CLIPPING WITH 3-DIMENSIONAL MODELS

OBJECTIVE: With improvements in endovascular techniques, fewer aneurysms are treated by surgical clipping, and those aneurysms targeted for open surgery are often complex and difficult to treat. We devised a hollow, 3-dimensional (3D) model of individual cerebral aneurysms for preoperative simulation and surgical training. The methods and initial experience with this model system are presented.

METHODS: The 3D hollow aneurysm models of 3 retrospective and 8 prospective cases were made with a prototyping technique according to data from 3D computed tomographic angiograms of each patient. Commercially available titanium clips used in our routine surgery were applied, and the internal lumen was observed with an endoscope to confirm the patency of parent vessels. The actual surgery was performed later.

RESULTS: In the 8 prospective cases, the clips were applied during surgery in the same direction and configuration as in the preoperative simulation. Fine adjustments were necessary in each case, and 2 patients needed additional clips to occlude the atherosclerotic aneurysmal wall. With these 3D models, it was easy for neurosurgical trainees to grasp the vascular configuration and the concept of neck occlusion. Practicing surgery with these models also improved their handling of the instruments used during aneurysm surgery, such as clips and appliers.

CONCLUSION: Using the hollow 3D models to simulate clipping preoperatively, we could treat the aneurysms confidently during live surgery. These models allow easy and concrete recognition of the 3D configuration of aneurysms and parent vessels.

KEY WORDS: Cerebral aneurysm, Clipping, Surgical simulation, Surgical training, 3-dimensional modeling

Neurosurgery 65:719–726, 2009 DOI: 10.1227/01.NEU.0000354350.88899.07 www.neurosurgery-online.com

Microsurgical clipping is the standard technique for cerebral aneurysm surgery. Since the International Subarachnoid Aneurysm Trial (8), and with improvements in endovascular techniques, cerebral aneurysms are increasingly treated through endovascular embolization (4). However, aneurysms that are not suited for endovascular intervention are often difficult to treat and are targeted for microsurgical treatment (1). Because the total number of aneurysms treated through clipping is decreasing, and aneurysms targeted for surgery are often of complex shape, there is a need for effective microsurgical training and a simulation system to practice clipping.

With the development of information technology, virtual reality simulation has been adopted by the field of microneurosurgery (6). The technology can show 3-dimensional (3D) views of cerebral vessels and aneurysms from various angles, and even clips and clip appliers, in the virtual monitor (13). Such image simulation can improve our concepts of aneurysm configuration and approach selection. Live surgery, however, presents various difficulties in handling aneurysms, such as how to occlude aneurysms without stenosis or kinking of the parent artery, the occlusion of perforating vessels or remnants of the aneurysm, and how to apply multiple clips for satisfactory clipping. Also, actual haptic feedback during the procedure is very important in learning skills.

ABBREVIATIONS: CTA, computed tomographic angiography; DICOM, Digital Imaging and Communication in Medicine; 3D, 3-dimensional

Supplemental digital content is available for this article. Direct URL citations appear in the printed text and are provided in the HTML and PDF versions of this article on the journal's Web site (www.neurosurgery-online.com).

We have developed 3D aneurysm models that are hollow and semielastic from individual patients' images, enabling surgical simulation and actual clip application using real aneurysm surgery equipment. Herein, we describe the development of this technique and initial experience with clinical cases.

MATERIALS AND METHODS

Aneurysm Model

Our 3D elastic hollow models were created with a soft, rubber-like polymer (FullCure 930 Tango Plus; Objet Geometries, Ltd., Rehovot, Israel; http://www.2objet.com/default.aspx) by using a rapid prototyping technology. Data acquired through Digital Imaging and Communication in Medicine (DICOM) from original, enhanced computed tomographic images of 3D computed tomographic angiography (CTA) were obtained for each patient. The data were transferred to the 3D calculation software, Mimics (Materialise Japan, Inc., Kanagawa, Japan; http://www.materialise.com/materialise/view/en/65854-Homepage.html). A virtual 3D angiogram was generated, and the vascular area of interest was segmented. Data from the segmented area were transformed into a stereolithographic format and transferred to MagicsRP (Materialise Japan, Inc.), in which the data are adjusted to fit the rapid prototyping machine. In this software, the vessel wall was created with a thickness of 0.3 or 0.5 mm over the vessel image from the CTA data because the original data showed contrast media inside the wall.

The data were then transformed into thin, virtual horizontal sections, and the rapid prototyping machine sprayed raw materials to make a 0.03-mm-thick layer of polymer (FullCure 930 Tango Plus). Then, ultraviolet light was used to harden the polymer according to the image of the vessel wall. The spray nozzle of the machine rises and the thin layer piles up to make the vessel wall. After the vessels of interest were built up, the contents, which were not hardened by the ultraviolet light, were curetted away manually to make the vessel hollow.

A hard bone model (KEZLEX; Ono & Co., Ltd., Tokyo, Japan; http://ono-and.com/) was made with the same technique, except that the polymer consisted of resin and talc, which become hard when irradiated, and the thickness of 1 layer of prototyping was 0.1 mm.

We created hollow 3D models for 3 retrospective cases and 7 prospective cases. Hard models were created for 1 retrospective case and 2 prospective cases. In the retrospective models, we assessed the most appropriate conditions for creating 3D models, such as the thickness of the aneurysm and arterial wall and the extent of the parent vessels needed for simulation.

The data processing and creation of the 3D models were done at the processing laboratory of Ono & Co., Ltd after we prepared 3D DICOM images from the patient's 3D CTA and marked the area we wanted to have as the 3D model. Currently, 3 to 7 days are needed to create the 3D model. Although this process was not a commercial enterprise of this company during the study, creating the model costs 300 to 400 United States dollars per patient according to the size and complexity of the aneurysm.

Surgical Simulation

We fixed the aneurysm model with either flexible wires or plastic clay in the direction of the surgical view, according to the approach selected for individual aneurysms. Then, under the operative microscope, we applied various types of aneurysm clips (Vasari Titanium Aneurysm Clips; Aesculap AG & Co. KG, Tuttlingen, Germany) until we determined satisfactory positions that did not occlude or kink the parent vessels and left as small a remnant as possible. The lumen of the aneurysms was checked with a thin, flexible vascular endoscope (Fig. 1, C and D) (DAG-2218LN; Machida Endoscope Co., Ltd., Tokyo, Japan).

When deciding the surgical approach, especially in patients with complex, deep-seated vertebrobasilar aneurysms, we used a hard 3D model including the aneurysm, vessels, and cranial base bone. By creating an actual craniotomy and drilling the skull base, we simulated the access to the aneurysms. In addition, by positioning the hollow 3D model in the same direction as the surgical approach, we could confirm whether clips could be applied through the corridor.

ILLUSTRATIVE CASES

Patient 3

A 64-year-old woman had a 10-mm unruptured anterior communicating artery aneurysm (Table 1). Her 2 sisters had been diagnosed with subarachnoid hemorrhage previously, and 1 of them died. Thus, this woman came to our hospital for surgical clipping. With the DICOM data from her 3D CTA, we prepared a hard KEZLEX model, including part of the skull, and an elastic soft aneurysm model. An interhemispheric approach and a right pterional approach were tried on the KEZLEX model (Fig. 2). We achieved optimal neck clipping through the right pterional craniotomy with a Yaşargil 10-mm straight clip combined with a fenestrated clip. The actual clipping of the patient's aneurysm was done through the right pterional approach, as practiced on the model (Fig. 1). During the simulation, we confirmed that the clipping occluded the aneurysmal neck completely by observing the intraarterial lumen through the microendoscope (Fig. 1, C and D). The patient's postoperative course was uneventful, and complete neck clipping was confirmed by 3D CTA.

Patient 5

A 61-year-old woman had an 11-mm aneurysm of the left middle cerebral artery (Table 1). She also had a family history of subarachnoid hemorrhage. During simulation on a soft aneurysm model, a curved clip (10.2 mm) was applied parallel to the M1–M2 bifurcation and combined with a fenestrated clip. During the actual operation, minor bleeding occurred when a small artery attached to the wall was dissected. The application of a single curved clip could not stop the bleeding because the neck was atherosclerotic and an additional clip was needed to stop the bleeding. A fenestrated clip was applied to occlude the residual neck, as was done in the simulation (Fig. 3). The patient's postoperative course was uneventful, and neck clipping was confirmed by 3D CTA as well.

Patient 6

A 63-year-old woman presented with a 22-mm aneurysm at the union of the vertebral arteries (Fig. 4; Table 1). See Video, Supplementary Digital Content 1, http://links.lww.com/A242, which demonstrates preoperative simulation and surgery in patient 6.) Using a hard KEZLEX model, we could drill the skull base and anticipate how much bone should be removed during surgery to expose the aneurysm neck appropriately. Also, using a soft elastic hollow model, we could apply various clips and decide which clip combination would be suitable to obliterate the aneurysm without inflow vessel occlusion. Actual surgery was done as planned during hard model simulation. We performed a left suboccipital and temporal craniotomy and exposed the aneurysm dome and neck, respectively. We placed clip grafts through the anterior petrosal route as had been planned in the soft model simulation.) A hard KEZLEX model and a soft aneurysm

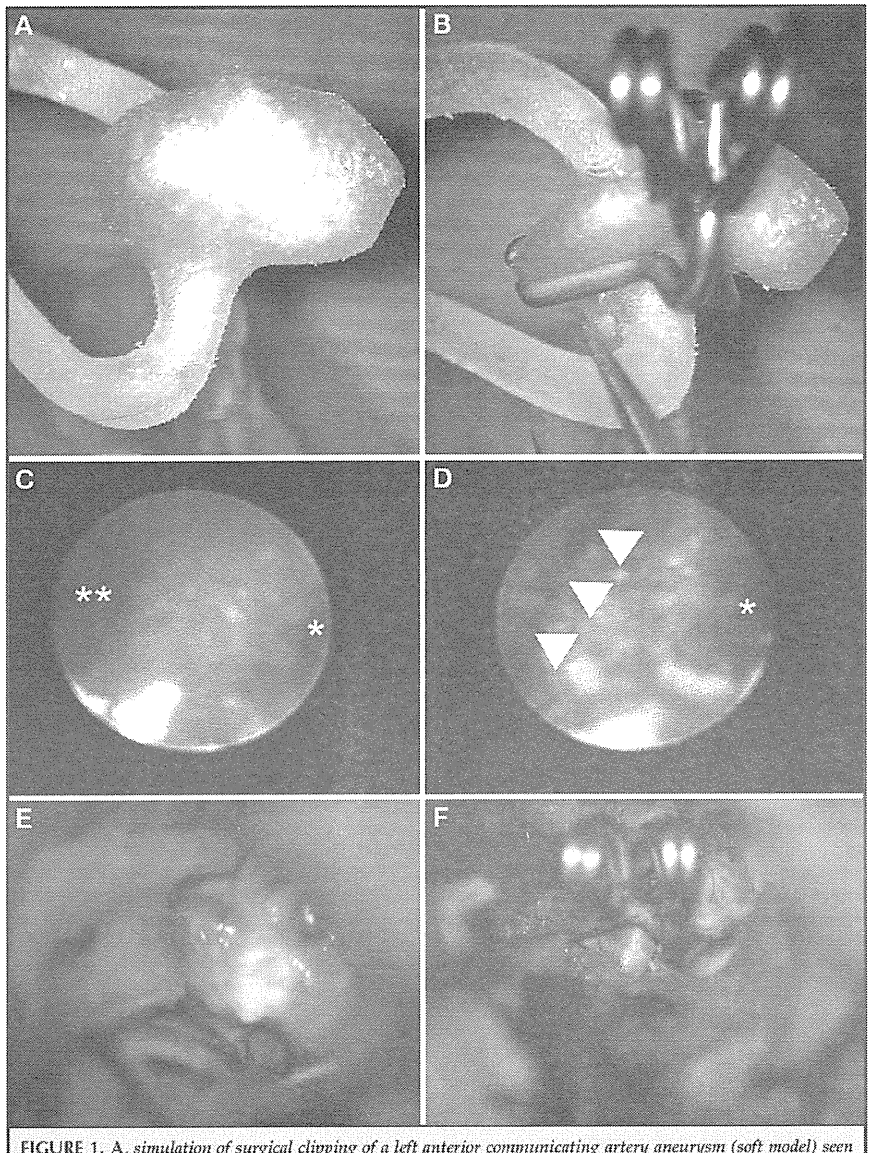

FIGURE 1. A, *simulation of surgical clipping of a left anterior communicating artery aneurysm (soft model) seen from the right pterional view.* B, *the ideal clipping—a straight clip combined with a fenestrated, bent clip.* C, *endoscopic view of the model seen from the left A2. The double asterisks show the aneurysm's orifice and the single asterisk shows the dominant left A1 orifice.* D, *after clipping simulation. The arrowheads show the closure line of the aneurysmal neck from inside the artery whereas the single asterisk shows patency and no stenosis of the parent A1.* E, *actual operative view of the aneurysm during the right pterional approach.* F, *after clipping. The aneurysm is obliterated as shown in the simulation.*

model were manufactured. Anterior petrosectomy was performed on the KEZLEX model, and the aneurysm neck was observed through this corridor. It was possible to apply clips through the window, but it seemed difficult to control the proximal vertebral artery. Therefore, in the actual surgery, a suboccipital craniotomy was added to prepare the proximal vertebral arteries. Although a 20-mm straight clip seemed appropriate to occlude the aneurysm neck of the soft model, we examined whether an additional tandem clip could be applied through the window considering the thickness of the aneurysmal wall and the pressure of the real aneurysm. In the actual surgery, a 12-mm blade fenestrated clip was added tandemly and a booster clip was applied on the anticipated 20-mm straight clip. Obliteration of the aneurysm was confirmed by digital subtraction angiography. Two months after surgery, the patient was neurologically intact, but her hearing was sacrificed.

RESULTS

A summary of the cases and findings during simulation and actual surgery is provided in Table 1. For models of retrospective cases, we created small to medium aneurysms (<15 mm) with a thickness of 0.3 mm, and large aneurysms (>15 mm) with a thickness of 0.5 mm. To efficiently remove the contents of aneurysms, we needed to limit the length of the parent artery, but we also needed enough length to simulate surgery. Therefore, we chose to include at least 10 mm of the parent vessel.

With the models of prospective cases, we could repeatedly apply various types of clips and choose the most appropriate clips and approach before surgery. In patients whose aneurysm had a wide neck, we could visually assess how close to the parent vessel we could place the clip blade without occluding or kinking the vessels. In 5 of 8 patients, the same selection and config-

TABLE 1. Summary of patients with prospective clip simulation[a]

Patient no.	Age (y)/sex	Location	Size (mm)	Best configuration in simulation	Actual clipping	Reclipping	Residual neck
1	56/F	R MCA	4	Slightly curved	Same	No	No
2	81/F	R MCA	11	Straight + fenest.	Curved + fenest.	No	No
3	64/F	AComA	10	Straight + fenest.	Same	1	No
4	68/F	L IC PComA	9	Bayonet	Same	No	No
5	61/F	L MCA	10	Slightly curved + fenest.	Slightly curved ×2 + fenest.	Adjustment	No
6	63/F	VA union	22	Straight ×2	Straight + fenest.	5	+
7	39/M	M1 fusiform	12	Straight ×2 + fenest.	Fenest. ×3	6	No
8	67/F	AComA	6	Bayonet	Same	2	+

[a] R, right; MCA, middle cerebral artery; fenest., fenestrated clip; AComA, anterior communicating artery; L, left; IC, internal carotid; PComA, posterior communicating artery; VA, vertebral artery.

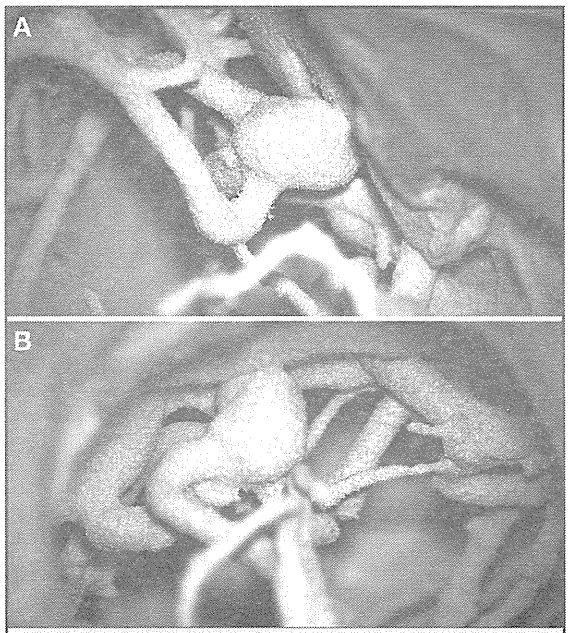

FIGURE 2. *Comparison of the surgical view of the anterior communicating artery aneurysm in case 1 using the hard KEZLEX (Ono & Co., Ltd., Tokyo, Japan) model. A, view from the right pterional craniotomy. B, during the interhemispheric approach.*

uration of clips were applied. In 1 patient with a medium-sized middle cerebral aneurysm (patient 5) and complex vertebrobasilar aneurysms (patient 6), we needed to apply additional clips to occlude the atherosclerotic aneurysmal neck. In a fusiform M1 aneurysm (patient 7), 3 ring clips were used to shape the artery, although a combination of a straight and a fenestrated clip seemed appropriate for shaping the middle cerebral artery during the preoperative simulation.

For help in selecting the surgical approach, we also created a hard artery and bone model to determine the most appropriate surgical access and bone removal. The most appropriate clip application was also assessed with the hollow model and a real clip. This concept was also used to decide the surgical approach to anterior communicating aneurysms (patient 3) and a vertebral artery union aneurysm (patient 6). In patient 3, by placing the aneurysms in the direction observed through either the interhemispheric or transsylvian approach, we could apply various clips and decide the approach or most appropriate clip combination. In patient 6, we knew whether the aneurysm neck could be dissected and the clip could be applied through the anterior petrosal corridor.

After the preoperative simulation was finished, the same models were used to train beginning neurosurgeons. With these models, they can learn how to handle clips and appliers, manipulate aneurysms, and place clips. By using the microendoscope, they can learn how the aneurysmal neck is occluded according to the direction of the clip. They can also recognize the importance of considering the intraluminal anatomy of the aneurysm and adjacent arteries during surgical repair.

DISCUSSION

With the development of embolizing materials and various techniques, endovascular treatment is becoming safer and more applicable to various types of cerebral aneurysms (8).

Now, more than 50% of aneurysms are considered manageable with endovascular treatment (4). However, some aneurysms are complex and difficult to treat through endovascular techniques that are often difficult for microsurgical clipping as well (1). The International Study of Unruptured Intracranial Aneurysms investigators showed that the rupture rate of

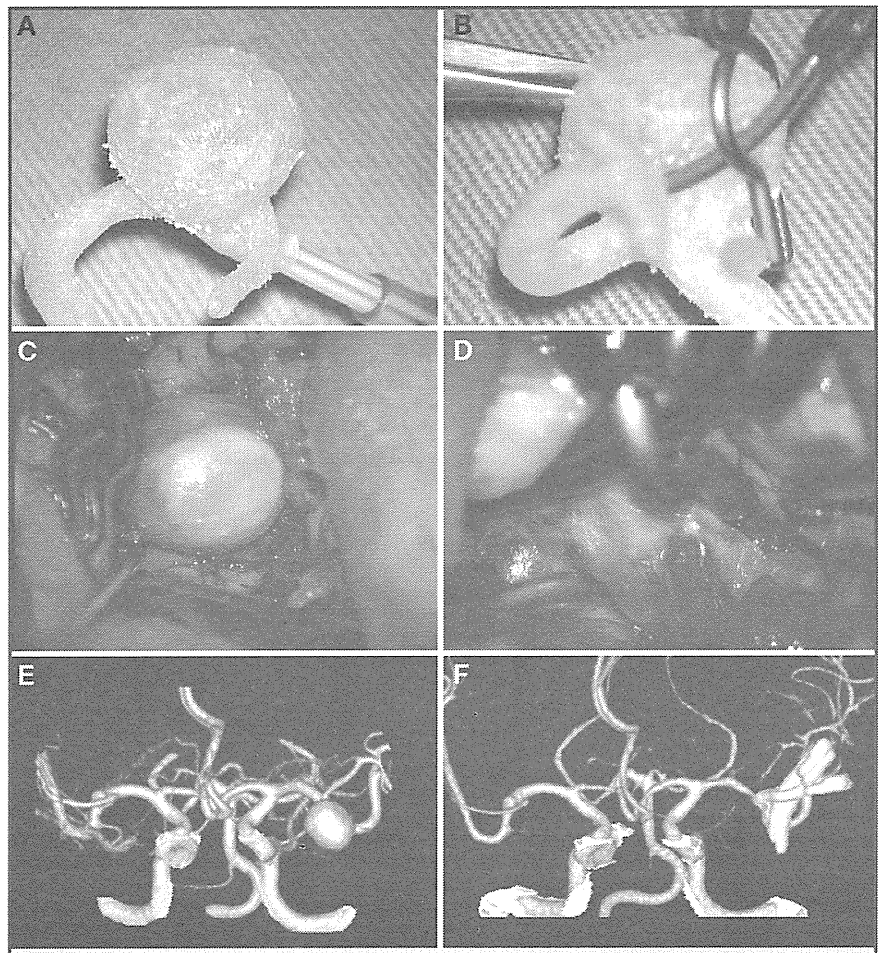

FIGURE 3. A, *left middle cerebral bifurcation aneurysm in a supposed surgical view.* B, *ideal clipping with a slightly curved clip combined with a fenestrated clip.* C, *actual operative view after sylvian dissection and elevation from the left frontal lobe.* D, *magnified view of the bifurcation after clipping. The configuration is the same as in the preoperative simulation, but 2 parallel clips were needed for sufficient closing pressure.* E, *preoperative 3-dimensional (3D) computed tomographic angiogram showing a large left middle cerebral artery aneurysm.* F, *postoperative 3D computed tomographic angiogram confirming satisfactory obliteration of the aneurysm.*

unruptured cerebral aneurysms depends on the size of the aneurysm. Small aneurysms are less often indicated for treatment, but larger aneurysms, with high surgical risks, are often indicated for surgery (12). With this scenario, the case load each neurosurgeon experiences is limited, and there are fewer chances to develop surgical skills in managing simple cerebral aneurysms (9). At the same time, neurosurgeons are faced with very difficult aneurysms needing surgical treatment. Therefore, there is a definite need for practical surgical simulation and an effective training system for aneurysm clipping procedures.

With the advancement of radiological modalities and information technology, 3D virtual reality models can be constructed on a personal computer (3, 7). More intricate images can be created on a workstation. As is prevalent in other fields of surgery, virtual reality training is being done on such applications as the Dextroscope (BRACCO AMT, Inc., Princeton, NJ) (11, 13). These 3D models help neurosurgeons grasp the 3D configuration of vascular anatomy both before and during surgery and make it easier to plan the operative procedure. However, in practical surgery, some difficulties are associated with vascular texture and distinct devices, specifically clips and clip appliers. The aneurysm and its parent artery change morphologically according to the application of the clip, but the virtual reality systems available today cannot yet provide sufficient images for each scenario and each aneurysm. Futami et al. (3) described simulating the positioning of a single straight clip on a workstation and assessed the aneurysmal remnant. This technique is very promising with further advancements in software, but it is not adequate for actual patients who require other or multiple types of clips.

Although an aneurysm clip and its applier are well designed for occlusion, a certain level of experience is necessary to handle these devices properly near the aneurysm, especially when reclipping or multiple clipping is needed. Although temporary clip systems are available, multiple reclipping in patients should be avoided because of the risk of premature rupture and inadvertent vessel injury.

Wurm et al. (14) reported on the utility of solid plastic models to grasp 3D anatomy of aneurysms. Because our 3D model is hollow and made of soft elastic silicone, the aneurysmal neck can be occluded with an actual aneurysm clip as is done during the actual operation, and we can assess the endoluminal

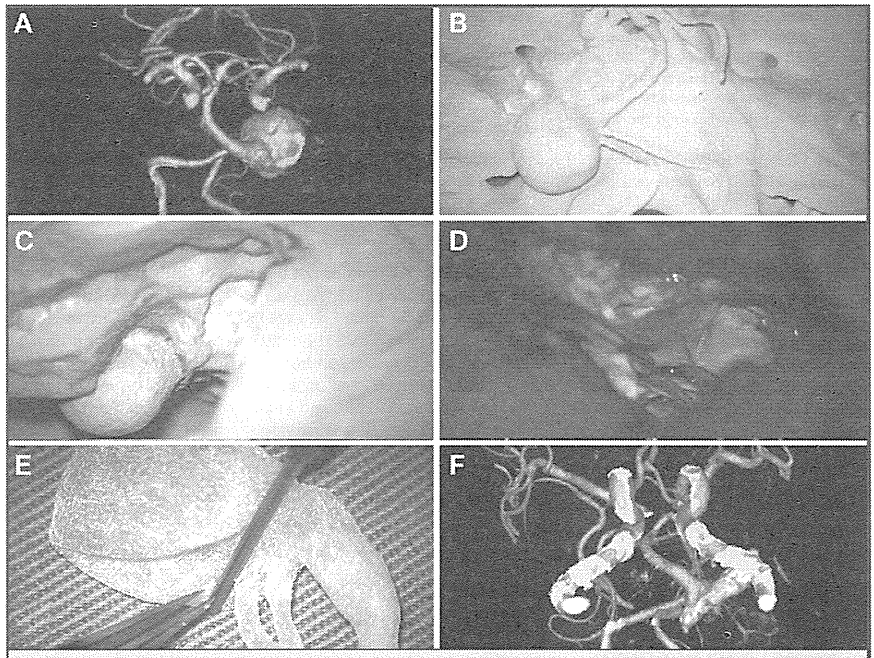

FIGURE 4. A, *vertebral artery union aneurysm projecting to the left.* B, *posterior view of the KEZLEX model after anterior petrosectomy and lateral suboccipital craniotomy. Anterior petrosal view of the KEZLEX model* (C), *and the actual aneurysm* (D). E, *clipping simulation on the soft model.* F, *postoperative computed tomographic angiogram.*

patency in addition to the ease of preoperative stereognostic understanding. Especially in complex cases, in which the aneurysm was large or had a wide neck, this model allowed us to estimate how close to the neck we could place the clip without occluding parent vessels. It also helped us to choose the best clip placement and combination to obliterate aneurysms. Our models were very similar to the actual aneurysms and, in all 8 prospective cases, we could manage the real aneurysms with the same configuration of clips.

The purpose of this model is to simulate the surgical repair of aneurysms for training. Information regarding surrounding tissue, such as adjacent structures or the Sylvian fissure, is not provided. Such information should be well recognized on each patient's preoperative imaging, such as magnetic resonance imaging. In addition, the models are supplied only with short segments of the vessels around the aneurysms. Placing such models in the appropriate direction under the microscope during simulation is a critical step in understanding the aneurysm's configuration and selecting the appropriate surgical approach. Also, the use of instruments needs to be confined during the simulation according to anticipated limitations caused by the surrounding brain tissue.

With this model, surgeons who do not have sufficient experience with clipping can practice as many times as necessary to be confident to perform clipping on actual patients. In addition, they can practice on and examine difficult past cases and improve their skills. This model has also been used to explain surgery and surgical risks before obtaining informed consent from patients. With such a model, patients and their families can easily understand the surgery and its risks (5). In the future, this system will be used to simulate endovascular procedures for individual complex aneurysms requiring various devices.

There are, however, several aspects of the model that need improvement. Because our model takes several days to be prepared, it cannot be used to simulate emergent cases such as ruptured aneurysms. The model creation process should be simplified and quickened. Furthermore, as D'Urso et al. (2) and Wurm et al. (14) have noted previously, because this model is created with data from the aneurysmal cavity, the thickness or consistency of the wall is not reflected. In part because of this insufficiency, we needed to add an extra clip in our patient with middle cerebral and vertebral artery union aneurysm. In addition, the perforators in the model are too small to be made hollow, and surgeons still need to make conceptual images so that those perforators are not occluded during actual clipping. They must also confirm the patency through multiple methods, such as micro-Dopplers, intraoperative fluorescent angiography using indocyanine green, and electrophysiological monitoring (10).

Disclosure

Financial support was provided by the Japan National Cardiovascular Center for developing a risk communication tool for managing unruptured cerebral aneurysms (19-Kou-Junni-Hashimoto han, 2007, 2008) and an Advanced Medical & Pharmaceutical Research Grant (2007). The authors have no personal financial or institutional interest in any of the drugs, materials, or devices described in this article.

REFERENCES

1. Choudhari KA, Ramachandran MS, McCarron MO, Kaliaperumal C: Aneurysms unsuitable for endovascular intervention: Surgical outcome and management challenges over a 5-year period following International Subarachnoid Haemorrhage Trial (ISAT). Clin Neurol Neurosurg 109:868–875, 2007.
2. D'Urso PS, Thompson RG, Atkinson RL, Weidmann MJ, Redmond MJ, Hall BI, Jeavons SJ, Benson MD, Earwaker WJ: Cerebrovascular biomodelling: A technical note. Surg Neurol 52:490–500, 1999.

3. Futami K, Nakada M, Iwato M, Kita D, Miyamori T, Yamashita J: Simulation of clipping position for cerebral aneurysms using three-dimensional computed tomography angiography. Neurol Med Chir (Tokyo) 44:6–13, 2004.
4. Gnanalingham KK, Apostolopoulos V, Barazi S, O'Neill K: The impact of the international subarachnoid aneurysm trial (ISAT) on the management of aneurysmal subarachnoid haemorrhage in a neurosurgical unit in the UK. Clin Neurol Neurosurg 108:117–123, 2006.
5. King JT Jr, Horowitz MB, Bissonette DJ, Tsevat J, Roberts MS: What do patients with cerebral aneurysms know about their condition? Neurosurgery 58: 824–830, 2006.
6. Kockro RA, Serra L, Tseng-Tsai Y, Chan C, Yih-Yian S, Gim-Guan C, Lee E, Hoe LY, Hern N, Nowinski WL: Planning and simulation of neurosurgery in a virtual reality environment. Neurosurgery 46:118–137, 2000.
7. Koyama T, Okudera H, Kobayashi S: Computer-assisted geometric design of cerebral aneurysms for surgical simulation. Neurosurgery 36:541–547, 1995.
8. Molyneux AJ, Kerr RS, Yu LM, Clarke M, Sneade M, Yarnold JA, Sandercock P; International Subarachnoid Aneurysm Trial (ISAT) Collaborative Group: International Subarachnoid Aneurysm Trial (ISAT) of neurosurgical clipping versus endovascular coiling in 2143 patients with ruptured intracranial aneurysms: A randomised comparison of effects on survival, dependency, seizures, rebleeding, subgroups, and aneurysm occlusion. Lancet 366:809–817, 2005.
9. Morgan MK, Assaad NN, Davidson AS: How does the participation of a resident surgeon in procedures for small intracranial aneurysms impact patient outcome? J Neurosurg 106:961–964, 2007.
10. Raabe A, Nakaji P, Beck J, Kim LJ, Hsu FP, Kamerman JD, Seifert V, Spetzler RF: Prospective evaluation of surgical microscope-integrated intraoperative near-infrared indocyanine green videoangiography during aneurysm surgery. J Neurosurg 103:982–989, 2005.
11. Stadie AT, Kockro RA, Reisch R, Tropine A, Boor S, Stoeter P, Perneczky A: Virtual reality system for planning minimally invasive neurosurgery. Technical note. J Neurosurg 108:382–394, 2008.
12. Wiebers DO, Whisnant JP, Huston J 3rd, Meissner I, Brown RD Jr, Piepgras DG, Forbes GS, Thielen K, Nichols D, O'Fallon WM, Peacock J, Jaeger L, Kassell NF, Kongable-Beckman GL, Torner JC; International Study of Unruptured Intracranial Aneurysms Investigators: Unruptured intracranial aneurysms: Natural history, clinical outcome, and risks of surgical and endovascular treatment. Lancet 362:103–110, 2003.
13. Wong GK, Zhu CX, Ahuja AT, Poon WS: Craniotomy and clipping of intracranial aneurysm in a stereoscopic virtual reality environment. Neurosurgery 61:564–569, 2007.
14. Wurm G, Tomancok B, Pogady P, Holl K, Trenkler J: Cerebrovascular stereolithographic biomodeling for aneurysm surgery. Technical note. J Neurosurg 100:139–145, 2004.

Acknowledgments

The 3D aneurysm models were created in collaboration with Ono & Co., Ltd. We thank Mr. Hisayuki Sugiyama, B.A., and Mr. Kazuhide Ono, B.A., for their efforts in developing new models to fit our concept. We also thank Mrs. Julie Yamamoto, B.A., for her editorial assistance.

Supplemental digital content is available for this article. Direct URL citations appear in the printed text and are provided in the HTML and PDF versions of this article on the journal's Web site (www.neurosurgery-online.com).

COMMENTS

Kimura et al. used individual patients' images to develop 3-dimensional (3D) aneurysm models that are hollow and semielastic. The models can be used to simulate surgery and clip application. This article describes their use of this technique with clinical cases. Surgeons were able to plan preoperatively which clip to use and how to apply it. Their 3D model also includes a cranial base bone to evaluate the optimal surgical corridor. Placement of a clip also depends on the surrounding brain, nerves, and pliability of the vessels.

This model is unique in that the vessels and aneurysm are hollow, and an endoscope can be used to confirm patency of the parent vessel after clipping. We agree with the authors' belief that this is a useful tool for preoperative planning and for training and practice, especially in the current environment, in which aneurysms are being treated increasingly by endovascular methods.

Francisco Ponce
Robert F. Spetzler
Phoenix, Arizona

3D models and surgical simulation are important topics for resident training. Whether or not this type of simulation really is helpful for an experienced aneurysm surgeon is hard to quantify. The preliminary attempts at modeling explained in this study are intriguing, but there are very significant limitations, as the authors outline. The models are very time consuming and cumbersome to construct, and they are unlikely to be used on a routine basis in the present form. In these models, the aneurysm and vessel wall thickness is not accounted for; however, wall thickness may be a critical factor in choosing and positioning clips. More importantly, in this model, the presence of perforators is not accounted for. Sparing perforators and understanding perforator anatomy may be the most important aspect of safe aneurysm clipping.

Robert A. Solomon
New York, New York

The authors have presented a clever and innovative method of creating models of intracranial aneurysms based on preoperative 3D imaging studies. These models were used for both simulation of the actual operative procedure and for training residents and young surgeons. Although the technique of developing these models appears to be somewhat cumbersome and possibly expensive, the concept of generating 3D models for surgical training and practice is a sound one. As stated by the authors, the number of intracranial aneurysms undergoing surgical treatment has declined with the advent of endovascular therapy. Simultaneously, the complexity of those aneurysms coming to surgery is increasing. This challenges the skills of the cerebrovascular surgeon and creates difficulties in training the next generation of cerebrovascular surgeons. Additionally, restrictions on resident work hours make it even more challenging to expose neurosurgical residents to an adequate volume of complicated cases to prepare them for practice. The discipline of surgery is far behind other professions, such as the airline industry, in creating simulators for the purpose of training. This is a step in the right direction.

Daniel L. Barrow
Atlanta, Georgia

Endovascular case volume is increasing with better technology and new techniques. This evolution is decreasing open microsurgical case volume and increasing case complexity. Residents are exposed to fewer training cases, and their involvement in complex cases may be limited. Young aneurysm surgeons are struggling to advance their proficiency in this environment. This article describes a technique to manufacture soft rubber aneurysm models for surgical simulation that replicate a patient's individual anatomy. These models enable the neurosurgeon to decide on the optimal surgical approach, select the best clip configurations, practice the clip application, and examine the reconstructed aneurysm neck from outside and inside the arteries. This tool would undoubtedly be helpful with surgical preparation and with retrospective re-examination of complicated cases that were associated

with morbidity or poor results. Good aneurysm surgeons spend time before surgery studying their patient's aneurysm anatomy, usually on the computer screen with 3D computed tomographic angiography or catheter angiography. A thorough appreciation of specific anatomy facilitates the dissection and minimizes surprises intraoperatively. The busy neurosurgeon does not have time to wait for models to be built for simulation but creates these models in his head, with his mind's eye. These models can help residents to develop these spatial perspectives and preoperative habits. In the current environment of aneurysm scarcity, these models should become an integral teaching tool for residents to develop their surgical and analytical skills.

Michael T. Lawton
San Francisco, California

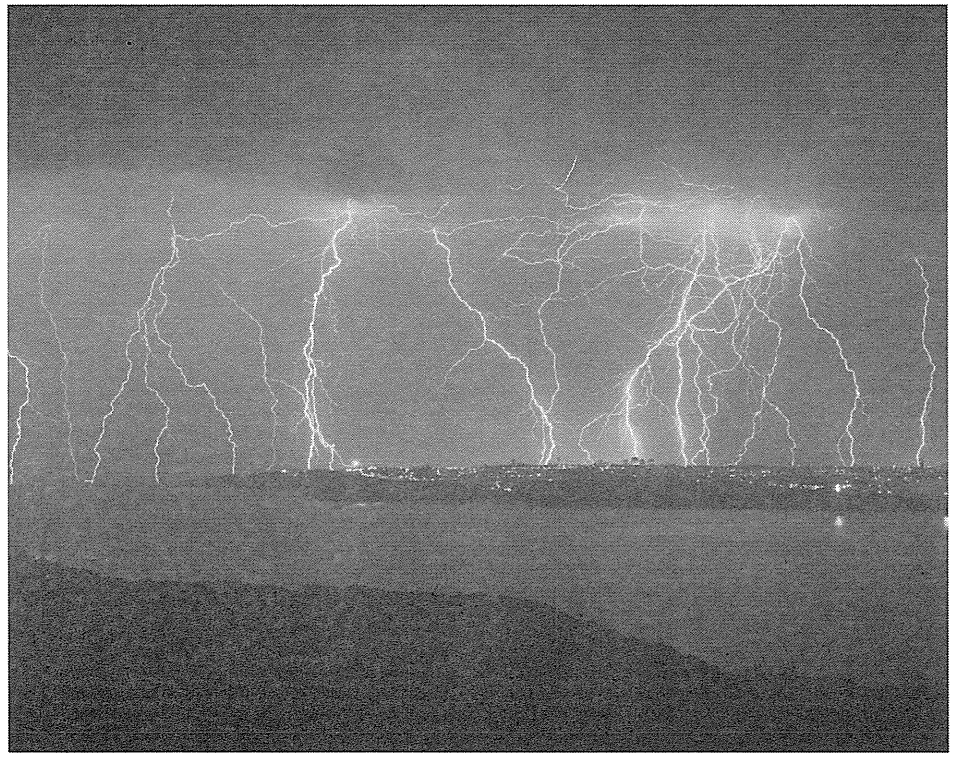

Fusiform Aneurysm of the Anterior Communicating Artery Treated by Vascular Reconstruction: Case Report

Toshikazu Kimura, MD
Department of Neurosurgery and Stroke Unit,
Kanto Medical Center,
NTT EC,
Tokyo, Japan

Kengo Nishimura, MD
Department of Neurosurgery and Stroke Unit,
Kanto Medical Center,
NTT EC,
Tokyo, Japan

Syunsuke Fukaya, MD
Department of Neurosurgery and Stroke Unit,
Kanto Medical Center,
NTT EC,
Tokyo, Japan

Akio Morita, PhD
Department of Neurosurgery and Stroke Unit,
Kanto Medical Center,
NTT EC,
Tokyo, Japan

Reprint requests:
Toshikazu Kimura, MD,
Department of Neurosurgery,
Kanto Medical Center, NTT EC.,
5-9-22, Higashigotannda,
Shinagawa-ku,
Tokyo, Japan 141-8625.
E-mail: tkim-tky@umin.ac.jp

Received, February 18, 2009,
Accepted, November 22, 2009.

OBJECTIVE: Fusiform aneurysm of the anterior cerebral artery is rare and difficult to treat because of perforators. We encountered a patient with subarachnoid hemorrhage due to rupture of a fusiform aneurysm of the anterior communicating artery complex, and treated this patient with cerebral revascularization.

CASE PRESENTATION: A 39-year-old man presented with sudden severe headache resulting from subarachnoid hemorrhage. Digital subtraction angiography showed dilatation from the distal A1 segment to the proximal A2 segment of the left anterior cerebral artery. Despite intensive conservative treatment, repetitive angiography showed aneurysmal growth from this dilated portion.

INTERVENTION: Proximal clipping and clip-on wrapping on the A2 segment was successfully performed with a A3-A3 bypass. He was discharged without neurological deficit.

CONCLUSION: Cerebral revascularization technique is necessary to achieved appropriate obliteration without ischemic complications.

KEY WORDS: A3-A3 bypass, Anterior cerebral artery, Anterior communicating artery, Fusiform aneurysm, Subarachnoid hemorrhage

Neurosurgery 66:E1025-E1026, 2010 DOI: 10.1227/01.NEU.0000367768.41781.CD www.neurosurgery-online.com

Intracranial fusiform aneurysm accounts for 1% of cerebral aneurysms and usually occurs in the vertebrobasilar artery, internal carotid artery, or middle cerebral artery. Fusiform aneurysm of the anterior cerebral artery (ACA) is rare and only 12 cases have been reported,[1-15] among which only 1 involved the anterior communicating artery (Acom).[8]

We performed cerebral revascularization by A3-A3 bypass to treat a patient with fusiform aneurysm of the Acom complex causing a subarachnoid hemorrhage.

CASE REPORT

An obese 39-year-old man presented to our hospital with severe headache. Cerebral computed tomography showed subarachnoid hemorrhage. Subsequent digital subtraction angiography (DSA) showed slight dilatation of the anterior cerebral artery from the distal A1 segment to the proximal A2 segment (Figure 1).

ABBREVIATIONS: ACA, anterior cerebral artery; **Acom,** anterior communicating artery; **DSA,** digital subtraction angiography.

There was a small notch behind the A1-A2 junction. Although the dilatation was suspected to be the bleeding point, we decided to observe the patient by controlling blood pressure and allowing bed rest; then, we repeated angiography to demonstrate the definitive bleeding source. Nine days later, on scheduled DSA, the notch had become larger and was confirmed to be the origin of hemorrhage. Because the lesion could have been a pseudoaneurysm protruding from the dissection of the anterior cerebral artery, we first established an A3-A3 bypass. Then, the interhemispheric fissure was opened to expose the anterior communicating artery complex. With gentle retraction of the left recral gyrus laterally, the left ACA was revealed to be red and dilated from the distal A1 to the proximal A2 segment, as shown on DSA. There was no evidence of wall dissection. A saccular protrusion was demonstrated behind the hypothalamic artery. We first occluded the left A1 segment distal to the perforator, and then clipped the saccular portion. Because the left recurrent artery originated from the dilated portion, trapping of the initial portion of A2 segment would have induced ischemic complication. Therefore, we wrapped the proximal A2 and clipped the arterial wall with a cellulose cotton sheet (Bemsheet®; Kawamoto, Osaka, Japan), maintaining the arterial lumen (Figure 2). The

patency of the hypothalamic and recurrent artery was confirmed by Doppler sonography (Figure 3). There was no paresis and the postoperative course was uneventful. The patient was discharged 22 days after surgery, following rehabilitation for disuse muscle atrophy. His intelligence quotient was 120 on discharge.

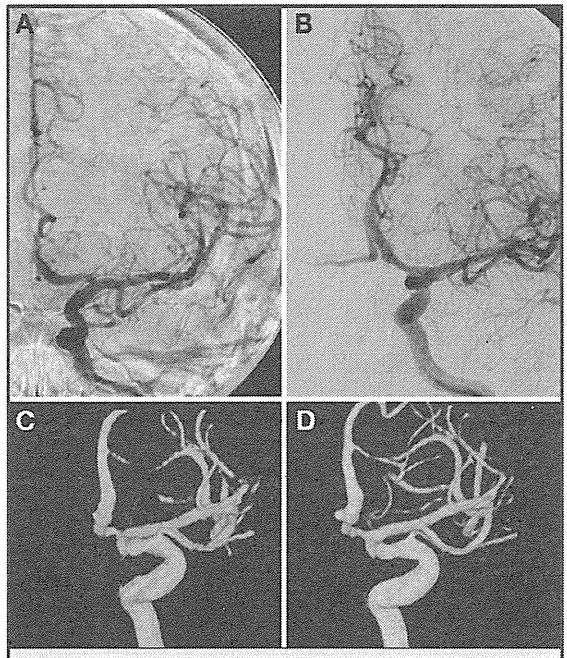

FIGURE 1. *Digital subtraction angiography on admission (A, C) and 9 days later (B, D). Aneurysmal growth was demonstrated behind the A1-A2 junction (D).*

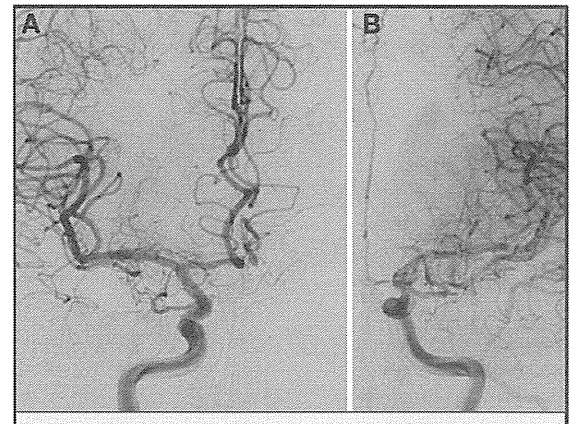

FIGURE 3. *Postoperative digital subtraction angiography demonstrated the obliteration of aneurysms and dilated parent artery, as well as the preservation of blood flow via an A3-A3 bypass.*

DISCUSSION

As the treatment of fusiform aneurysms, several options have been reported particularly for middle cerebral artery cases.[16-18] Trapping or excision, or induction of thrombosis by proximal clipping, with revascularization when needed, seems ideal when possible, because it can eliminate the affected artery from the circulation. Angioplastic clipping can preserve the blood flow, but is associated with technical difficulty; in addition, previous reports have mentioned the occurrence of rebleeding after clipping.[16,18] Simple proximal occlusion alone is sometimes used to reduce the pressure of the affected artery. Wrapping is used to reinforce the wall of the aneurysm.[19]

Fusiform aneurysm of the ACA is rare and only 20 cases have been reported previously (Table 1). Fourteen of those cases were restricted to the A1 segment. Among those reports with description of the treatment, 5 cases were treated by trapping, some of which sacrificed perforators, and 2 were treated by clipping of the aneurysm. In fusiform A1 cases, preserving the flow of distal ACA is mandatory and it depends on the collateral flow through the

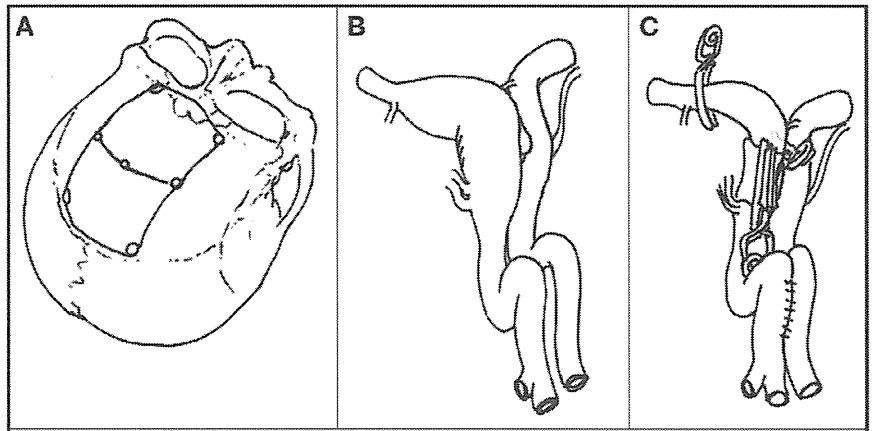

FIGURE 2. *A, schematic view of craniotomy. In addition to usual craniotomy for interhemispheric approach for the Acom complex, additional craniotomy was made to access to the genu of corpus callosum for A3-A3 bypass. B, illustration showing dilatation of the parent artery from distal A1 segment to proximal A2 segment. The left recurrent artery arises from the dilated portion of left A2 segment. C, schematic view after the procedure.*

TABLE 1. Reported Cases[a]

Author	Age	Sex	Laterality	Treatment	SAH	Outcome	SAH
Yaşargil (1984)[15]	64	F	Lt.	Trapping	+	Good	+
	54	F	Lt.	Trapping	+	Good	+
Nakasu et al (1984)[8]			Acom	Autopsy	+	Dead	+
Tamura et al (1985)[14]	54	M	Lt.	Clipping	–	good	–
Shigemori et al (1988)[11]	47	M	Lt.	Clipping	+	Good	+
Suzuki et al (1988)[13]	62	F	Lt.	ND	+	ND	+
Oba et al (1989)[10]	49	M	Lt.	Trapping	+	Good	+
	62	F	Lt	Conservative	+	Good	+
Suzuki et al (1992)[12]	49	M	Lt.	Trapping	+	ND	+
Nomura et al (2000)[9]	68	M	Lt.	Coiling	+	Good	+
Kashimura et al (2006)[6]	65	F	Rt.	STA-A1 bypass	+	Good (2)	+
Aoki et al (2007)[1]	42	M	Lt.	Trapping	+	Good	+
Present case	39	M	Lt.	Proximal occlusion +A3-A3 bypass	+	Good	+

[a] SAH, subarachnoid hemorrhage; Lt., left; Acom, anterior communicating artery; Rt., right; ND, not described.
In addition to these, Dashti et al described 6 cases of fusiform aneurysms of the anterior cerebral artery in the review of their database. Park et al reported 2 cases in their review.

Acom. In 1 case, STA-A1 end-to-end anastomosis was recruited after trapping and resection of the aneurysm as contralateral A1 was thin due to vasospasm.[6] In the review of their database, Dashti mentioned the use of an encircling Sundt clip to reshape the A1 segment,[20] which is associated with the risk of occlusion of the recurrent artery or perforators because of its awkwardness.

When the Acom complex is involved, as in our case, it becomes more difficult to manage the aneurysm because of the importance of the recurrent and hypothalamic arteries, which cannot be sacrificed. Only 4 cases of Acom fusiform aneurysm have been reported. One is an autopsy case,[8] and no details were described about the others.[5]

In our case, it seemed reasonable to manage the patient conservatively at first, because there was no obvious aneurysm other than dilatation of ACA. In previous reports of A1 segment aneurysms, 1 case was managed conservatively and demonstrated a good course.[10] However, the second DSA in the present case showed enlargement of the aneurysm and the risk of rebleeding was considered high. Therefore, radical treatment was needed. One choice might have been to clip only the saccular part, but there are reports describing rebleeding after simple clipping for fusiform aneurysms as mentioned above.[16,18] Furthermore, there was still a possibility that the saccular part on the DSA was a pseudoaneurysm originating from the dissecting aneurysm of ACA. It is difficult to distinguish fusiform aneurysm from dissecting aneurysm because the latter sometimes shows only dilatation of the affected artery. If there was dissection in the parent artery, the dissecting portion of ACA might need to be trapped, and extremely adverse ischemic complications would occur in the distal ACA area. To avoid this, we established an A3-A3 bypass as the first step, and then observed the Acom complex. The dilated portion of the ACA demonstrated a rather red wall, and there was no evidence of dissection. By occluding the A1 segment at just distal of the perforator, the fusiform part of the A1 became a blind end, and thrombosed. We planned to trap the dilated portion if possible, but because the recurrent arteries and the hypothalamic artery both originated from the dilated portion, we reinforced the proximal A2 portion by a clip-on-wrapping method.

Although there is no report concerning clip-on-wrapping of ACA fusiform aneurysm, the possibility of regrowth of the aneurysm or rebleeding remains, and careful observation with conventional DSA is needed to check the internal cavity, excluding the artifact of the clips, as the abnormal A2 segment is not excluded from the circulation.

In 11 of 14 cases, in which the detail of the aneurysms were described, the lesions originated from the left A1 segment. Although there is not sufficient information about the contralateral A1 segment, this predominance may be related to anatomic dominance or embryological origin.

In the management of ruptured fusiform aneurysm of relatively large arteries such as vertebral or internal carotid arteries, meticulous endovascular management including stent with coil method or flow diversion technique using Pipeline Embolization Device (PED; Chestnut Medical, Menlo Park, CA) can be a choice of treatment with good patency of the perforators,[20] but the current technique and the management of fine vessel disease with endovascular stenting carries high risks of complications by thromboembolic events or by hemorrhagic state due to its necessity of intraoperative anticoagulation and pre- and postprocedural antiplatelet regimen. An open surgery technique including deep vessel reconstruction is needed to manage complex cerebrovascular disease with a satisfactory outcome.

Disclosure

The authors have no personal financial or institutional interest in any of the drugs, materials, or devices described in this article.

REFERENCES

1. Aoki Y, Nemoto M, Yokota K, Kano T, Goto S, Sugo N. Ruptured fusiform aneurysm of the proximal anterior cerebral artery (A1 segment). *Neurol Med Chir (Tokyo).* 2007;47(8):351-355.
2. Bromowicz J, Danilewicz B, Jedlińska M. Subarachnoid hemorrhage from a fusiform aneurysm of the anterior cerebral artery [in Polish]. *Neurol Neurochir Pol.* 1984; 18(4):383-386.
3. Dashti R, Hernesniemi J, Lehto H, et al. Microneurosurgical management of proximal anterior cerebral artery aneurysms. *Surg Neurol.* 2007;68(4):366-377.
4. Evans AL, Corkill RA, Wenderoth JD. Ruptured fusiform aneurysm of fenestrated A1 segment of the anterior cerebral artery. Case report and review of the literature. *Neuroradiology.* 2006;48(3):196-199.
5. Hernesniemi JA, Dashti R, Lehecka M, et al. Microneurosurgical management of anterior communicating artery aneurysms. *Surg Neurol.* 2008;70(1):8-29.
6. Kashimura H, Mase T, Ogasawara K, Ogawa A, Endo H. Trapping and vascular reconstruction for ruptured fusiform aneurysm in the proximal A1 segment of the anterior cerebral artery. *Neurol Med Chir (Tokyo).* 2006;46(7):340-343.
7. Lehecka M, Dashti R, Hernesniemi J, et al. Microneurosurgical management of aneurysms at the A2 segment of anterior cerebral artery (proximal pericallosal artery) and its frontobasal branches. *Surg Neurol.* 2008;70(3):232-246.
8. Nakasu Y, Saito A, Handa J. Fusiform aneurysm of the anterior communicating artery. *Surg Neurol.* 1984;21(5):511-514.
9. Nomura M, Kida S, Kita D, et al. Fusiform aneurysm of the proximal anterior cerebral artery (A1). *Acta Neurochir (Wien).* 2000;142(10):1163-1164.
10. Oba M, Suzuki M, Onuma T. Two cases of ruptured fusiform aneurysm of the proximal anterior cerebral artery (A1 segment) [in Japanese]. *No Shinkei Geka.* 1989; 17(4):365-368.
11. Shigemori M, Kawaba T, Yoshitake Y, Miyagi J, Kuramoto S. Fusiform aneurysm of the proximal anterior cerebral artery. *J Neurol Neurosurg Psychiatry.* 1988;51(3):451.
12. Suzuki M, Onuma T, Sakurai Y, Mizoi K, Ogawa A, Yoshimoto T. Aneurysms arising from the proximal (A1) segment of the anterior cerebral artery: a study of 38 cases. *J Neurosurg.* 1992;76(3):455-458.
13. Suzuki M, Onuma T, Sakurai Y, Suzuki J. Twenty-six cases regarding the proximal anterior cerebral artery [in Japanese]. *No Shinkei Geka.* 1988;16(6):701-705.
14. Tamura M, Tsukahara Y, Yodonawa M. Fusiform aneurysm of the anterior cerebral artery (A1 segment): a case report [in Japanese]. *No Shinkei Geka.* 1985;13(12): 1337-1340.
15. Yaşargil MG. Anterior cerebral and anterior comunicating artery aneurysm. In: Yaşargil MG, ed. *Microneurosurgery.* Vol 2. Stuttgart: Georg Thieme Verlag; 1984:165-231.
16. Day AL, Gaposchkin CG, Yu CJ, Rivet DJ, Dacey RG Jr. Spontaneous fusiform middle cerebral artery aneurysms: characteristics and a proposed mechanism of formation. *J Neurosurg.* 2003;99(2):228-240.
17. Horie N, Takahashi N, Furuichi S, et al. Giant fusiform aneurysms in the middle cerebral artery presenting with hemorrhages of different origins: report of three cases and review of the literature. *J Neurosurg.* 2003;99(2):391-396.
18. Park SH, Yim MB, Lee CY, Kim E, Son EI. Intracranial fusiform aneurysms: it's pathogenesis, clinical characteristics and managements. *J Korean Neurosurg Soc.* 2008;44(3):116-123.
19. Sadasivan B, Ma S, Dujovny M, Ho LK, Ausman JI. Use of experimental aneurysms to evaluate wrapping materials. *Surg Neurol.* 1990;34(1):3-7.
20. Fiorella D, Woo HH, Albuquerque FC, Nelson PK. Definitive reconstruction of circumferential, fusiform intracranial aneurysms with the pipeline embolization device. *Neurosurgery.* 2008;62(5):1115-1121.

Role of Shear Stress in the Blister Formation of Cerebral Aneurysms

Masaaki Shojima, MD, PhD
Department of Neurosurgery,
The University of Tokyo,
Tokyo, Japan; and
Department of Endovascular Neurosurgery,
Jichi Medical University Hospital,
Tochigi, Japan

Shigeru Nemoto, MD, PhD
Department of Endovascular Neurosurgery,
Jichi Medical University Hospital,
Tochigi, Japan

Akio Morita, MD, PhD
Department of Neurosurgery,
NTT East Kanto Medical Center,
Tokyo, Japan

Marie Oshima, PhD
Institute of Industrial Science,
The University of Tokyo,
Tokyo, Japan

Eiju Watanabe, MD, PhD
Department of Neurosurgery,
Jichi Medical University,
Tochigi, Japan

Nobuhito Saito, MD, PhD
Department of Neurosurgery,
The University of Tokyo,
Tokyo, Japan

Reprint requests:
Masaaki Shojima, MD, PhD,
Department of Neurosurgery,
The University of Tokyo,
7-3-1 Hongo, Bunkyo-ku,
Tokyo 113-8655, Japan.
E-mail: mshoji-tky@umin.ac.jp

Received, August 12, 2009.
Accepted, January 11, 2010.

BACKGROUND: The development of cerebral aneurysms is related to hemodynamic stress.

OBJECTIVE: To elucidate the role of shear stress in the blister formation of cerebral aneurysms.

METHODS: Among 82 aneurysms detected during catheter-based 3D rotational angiography (3DRA), 4 aneurysms enlarged with blister formation during a mean follow-up period of 10.1 month. Three of these 4 aneurysms were analyzed in this study. The regions of blister formation were characterized by comparing 3DRA before and after blister formation, and computational fluid dynamic simulations were performed based on the aneurysm geometry before blister formation.

RESULTS: The spatially averaged shear magnitude was lower in the aneurysm region (0.97 ± 0.39 Pa) than in the parent artery (2.75 ± 0.92 Pa). The spatially averaged shear magnitude of the blister-forming area was extremely low (0.48 ± 0.12 Pa), and the shear magnitude dropped precipitately to subphysiological levels, resulting in a high shear gradient near the border of the blister-forming area.

CONCLUSION: These data suggest that low shear magnitude may trigger the progression of cerebral aneurysms and that blister formation is associated with high shear gradient in the large region of low shear magnitude on the aneurysm wall.

KEY WORDS: Biomechanics, Computer simulation, Hemodynamics, Intracranial aneurysm, Shear stress

Neurosurgery 67:1268–1275, 2010 DOI: 10.1227/NEU.0b013e3181f2f442 www.neurosurgery-online.com

Cerebral aneurysms typically arise at vascular branch points, most likely because of alterations in hemodynamic forces at these points. High and supraphysiological shear magnitudes lead to fragmentation of the internal elastic lamina,[1] thereby promoting aneurysm formation.[2]

However, the role of shear stress on aneurysm progression remains unclear. Intuitively, high shear magnitude would be expected to promote the enlargement and rupture of cerebral aneurysms, because that promotes the formation of cerebral aneurysms. However, the cellular and hemodynamic mechanisms related to aneurysm progression may differ from those involved in the aneurysm formation.[3,4] Several studies suggest that low shear magnitude might trigger aneurysm progression and eventual rupture.[5-7]

Our group has observed rare cases of aneurysms with subsequent blister formation leading to enlargement or rupture. Detailed 3-dimensional (3D) images were obtained before and after the blister formation in these cases. In the present study, computational fluid dynamic simulations were performed based on the aneurysm geometry before blister formation to characterize the hemodynamic features associated with the subsequent blister formation on cerebral aneurysms.

ABBREVIATIONS: AcomA, anterior communicating artery; **3D,** 3-dimensional; **3DRA,** 3D rotational angiography; **MCA,** middle cerebral artery

MATERIALS AND METHODS

Patient Population

From March 2007 to August 2008, 119 unruptured cerebral aneurysms among 93 patients were characterized with catheter angiography and 3D rotational angiography (3DRA) at Jichi Medical University Hospital. Within this population, 82

aneurysms among 62 patients were followed with magnetic resonance angiography over a mean period of 10.1 months (range, 1–25 mo). Among the cases with blister formation, 2 aneurysms enlarged and 2 aneurysms ruptured during the observation period. One anterior communicating artery (AComA) aneurysm that enlarged 17 months after the initial 3DRA was excluded from final analysis because the aneurysm was supplied by both anterior cerebral arteries and because 3DRA data quality was insufficient for fluid dynamic simulation. Thus, a total of 3 aneurysms were subjected to computational fluid dynamic simulation (Table).

Vessel and Aneurysm Modeling

Three-dimensional rotational angiography was performed using a C-arm angiography unit with flat detectors (Allura Xper FD 20/10; Philips Medical Systems, Best, Netherlands). During the 180°C-arm rotation, contrast medium (300 mgI/mL) was injected at a rate of 4 mL/s for 5 seconds via a catheter placed at the internal or vertebral artery, and 120 angiographic images with a matrix size of 1024 × 1024 pixels were obtained with a 17-inch field of view. These images were converted to isotropic 3D volume data with a voxel size of 0.28 mm in the equipped workstation.

Vessels and aneurysms were segmented by adjusting the threshold curve of the volume-rendered image on the workstation, resulting in the output of 3D surfaces. Thresholds were adjusted to keep the same reference diameter (ie, the diameter of the parent artery) when comparing images before and after the blister formation, thereby ensuring a consistent threshold policy.

The 3D surface was processed using a preprocessor equipped with a finite volume solver, SC/Tetra (Software Cradle, Osaka, Japan), to refine the fine irregularities of the 3D surfaces, to make planes for inlets and outlets, and to clear small branches from the region of interest. The computational meshes generated for the aneurysms before the blister formation consisted of 545 690 tetrahedral elements and the average resolution of the meshes was 0.32 mm. Regions of analysis encompassed the area from the cavernous segment of the internal carotid artery (cases 1 and 2) or from both of the vertebral arteries (case 3) to segments at least 15 mm distal to the aneurysms.

TABLE. Subject Characteristics and Results of Fluid Dynamic Simulation[a]

	Case		
	1	2	3
Age, y	58	49	59
Sex	Female	Female	Male
Aneurysm site	Left MCA	AComA	BA
Size, mm			
Before BF	3.8	6.6	9.7
After BF	5.7	7.1	9.7
Event	Enlargement	Rupture	Rupture
Interval, mo	15	2	1
Flow rate at inlets, mL/min	230	212	130
Reynolds number	322	191	189
Womersley number	2.53	2.35	1.95
Shear magnitude, Pa			
Parent artery	3.28	3.29	1.69
Whole aneurysm	1.41	0.69	0.80
Blister forming area	0.61	0.40	0.42

[a]MCA, middle cerebral artery; AComA, anterior communicating artery; BA, basilar artery; BF, blister formation.

Numerical Simulations

For aneurysm geometry before blister formation, 3D pulsatile blood flow was modeled with a finite volume solver (SC/Tetra) under governing equations of mass conservation and Navier-Stokes.

The flow rate and waveform at each of the inlets were derived from each case within 1 month after blister formation using phase contrast magnetic resonance velocimetry. Measured flow rates were imposed on the cross-sectional area of the inlets as velocity inlet conditions according to Womersley's analytic solution of oscillatory flow.[8] The average of the Reynolds number and Womersley number at the parent arteries of the aneurysms were 234 and 2.28, respectively, and laminar flow conditions were assumed for the fluid dynamic simulations.

Blood was assumed to be an incompressible Newtonian fluid with a specific gravity of 1053 kg/m^3 and a viscosity of 4.0×10^{-3} N/m^2·s. The viscoelastic properties of the vessel walls were neglected and a rigid wall with a no-slip condition was assumed. Zero surface pressure was applied for the outlet boundaries.

The width of the time step for the calculation was adjusted by the solver to control the Courant number to <1. To confirm numerical stability, calculations were performed for 5 cardiac cycles, and the results from the 5th cycle were used for analysis.

Data Analysis

The area of blister formation on the aneurysm wall was determined precisely by overlaying the 3D surfaces before and after the blister formation using Avizo 5 (Mercury Computer and Systems, Inc., Chelmsford, Massachusetts). Coregistration of the 3D surfaces was performed in a semiautomatic fashion according to the normalized mutual information-based algorithm (Figure 1).

All instantaneous velocity fields calculated during 1 cardiac cycle were averaged to create time-averaged velocity fields for each case and the streamlines and the spatial distributions of shear magnitude were visualized using postprocessing software equipped with SC/Tetra. Results were analyzed with particular interest to the area of eventual blister formation. Shear magnitude of 1 to 7 N/m^2 [Pa] was considered as physiological in this study.[9]

RESULTS

Results of the fluid dynamic simulations are summarized in the Table.

The shear magnitude of the aneurysm region was within or lower than the physiological level (1-7 Pa) except for case 1, in which a small area with high shear magnitude >7 Pa was observed at the neck of the aneurysm. The shear magnitude of the whole aneurysm region was low (mean ± standard deviation, 0.97 ± 0.39 Pa) in all 3 cases when compared with the shear magnitude of the parent artery (2.75 ± 0.92 Pa). The shear magnitude dropped precipitately to the subphysiological level (ie, below 1 Pa) near the border of the blister-forming area, and the spatially averaged shear magnitude of the blister-forming area was extremely low (0.48 ± 0.12 Pa).

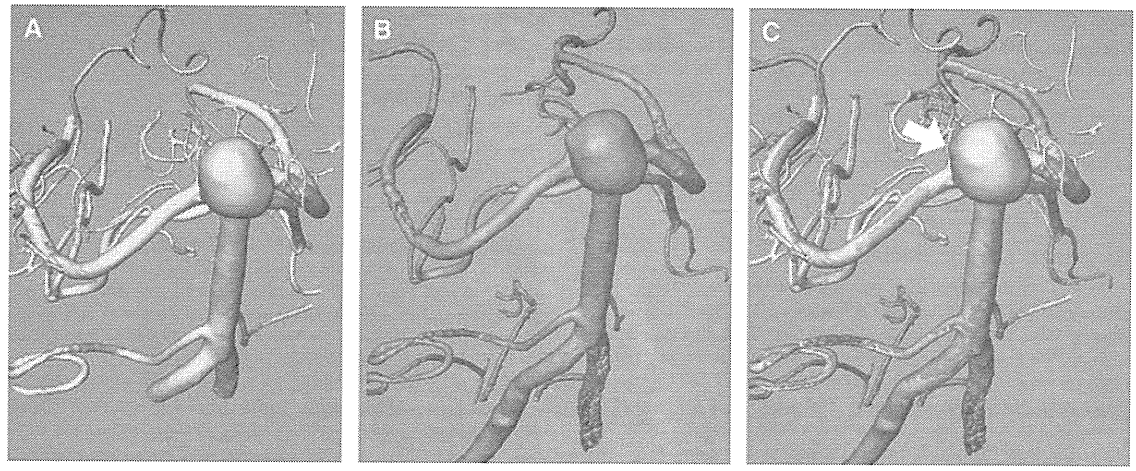

FIGURE 1. *Coregistration of 3D surfaces before and after blister formation Three-dimensional surfaces before (A) and after (B) blister formation were coregistrated in a semiautomatic fashion using Avizo 5 based on the normalized mutual information-based algorithm (C). White arrow indicates the location of blister formation.*

Case 1 (Figure 2)

An unruptured left middle cerebral artery (MCA) aneurysm (size 3.8 mm) in a 58-year-old female enlarged 15 months after initial 3DRA. Magnetic resonance angiography was obtained every 5 months, and no changes in size or shape were documented until the last examination. Repeat 3DRA showed aneurysm enlargement to 5.7 mm. Deformation was noted only in the upper portion of the aneurysm. The bloodstream of the parent artery did not impinge directly against the area of subsequent blister formation.

The spatially averaged shear magnitude of the blister-forming area was extremely low (0.61 Pa). The shear magnitude was moderately elevated in the area adjacent to the blister formation, and it dropped precipitately to subphysiological level (<1 Pa) near the border of the blister-forming area.

Case 2 (Figure 3)

A 49-year-old female with 2 unruptured aneurysms at the AComA (6.6 mm) and the left MCA (10.3 mm) developed subarachnoid hemorrhage 2 months after initial 3DRA. Repeated 3DRA after bleeding revealed newly formed blisters in the AComA aneurysm, which was confirmed as the culprit lesion during surgical clipping of both aneurysms. This AComA aneurysm was supplied by the left anterior cerebral artery.

Blood inflow from the parent artery was directed against the right lateral wall of the aneurysm, resulting in moderately elevated shear magnitude within physiological levels (~2 Pa), and the shear magnitude decreased to a subphysiological level (<1 Pa) near the border of the blister-forming area. The region of subsequent blister formation was located at the top of the aneurysm, where the shear magnitude was extremely low (0.40 Pa).

Case 3 (Figure 4)

A 59-year-old male with an unruptured basilar-tip aneurysm (size, 9.7 mm) developed a subarachnoid hemorrhage 1 month after initial catheter angiography and 3DRA. At repeat catheter angiography, no other aneurysms were documented, and 3DRA after bleeding showed a small, newly formed blister on the right posterolateral aspect of the aneurysm. Thus, this aneurysm was presumed to be the culprit lesion.

The bloodstream from the basilar artery entered into the aneurysm from the right side, creating an area of shear magnitude of approximately 3 Pa. The spatially averaged shear magnitude of the blister-forming area was extremely low (0.42 Pa).

DISCUSSION

In the present study, computational fluid dynamic simulations were used to characterize 3 aneurysms that enlarged or ruptured with blister formation during the observation periods. The shear magnitude dropped precipitately to subphysiological levels near the border of the blister-forming area, and blister formation occurred in the area with low shear magnitude.

Intuitively, high shear magnitude would be expected to promote the enlargement and rupture of cerebral aneurysms, because that promotes the formation of cerebral aneurysms. However, the shear magnitude of the area of subsequent blister formation was low in the subphysiological level in this study. This could be explained by the role of low shear magnitude in the endothelial functions and in the vascular disease processes. Prolonged nonphysiological shear conditions, including either excessively high or excessively low shear magnitude, may trigger vascular disease processes.[9,10] High shear magnitude near the vessel branch points

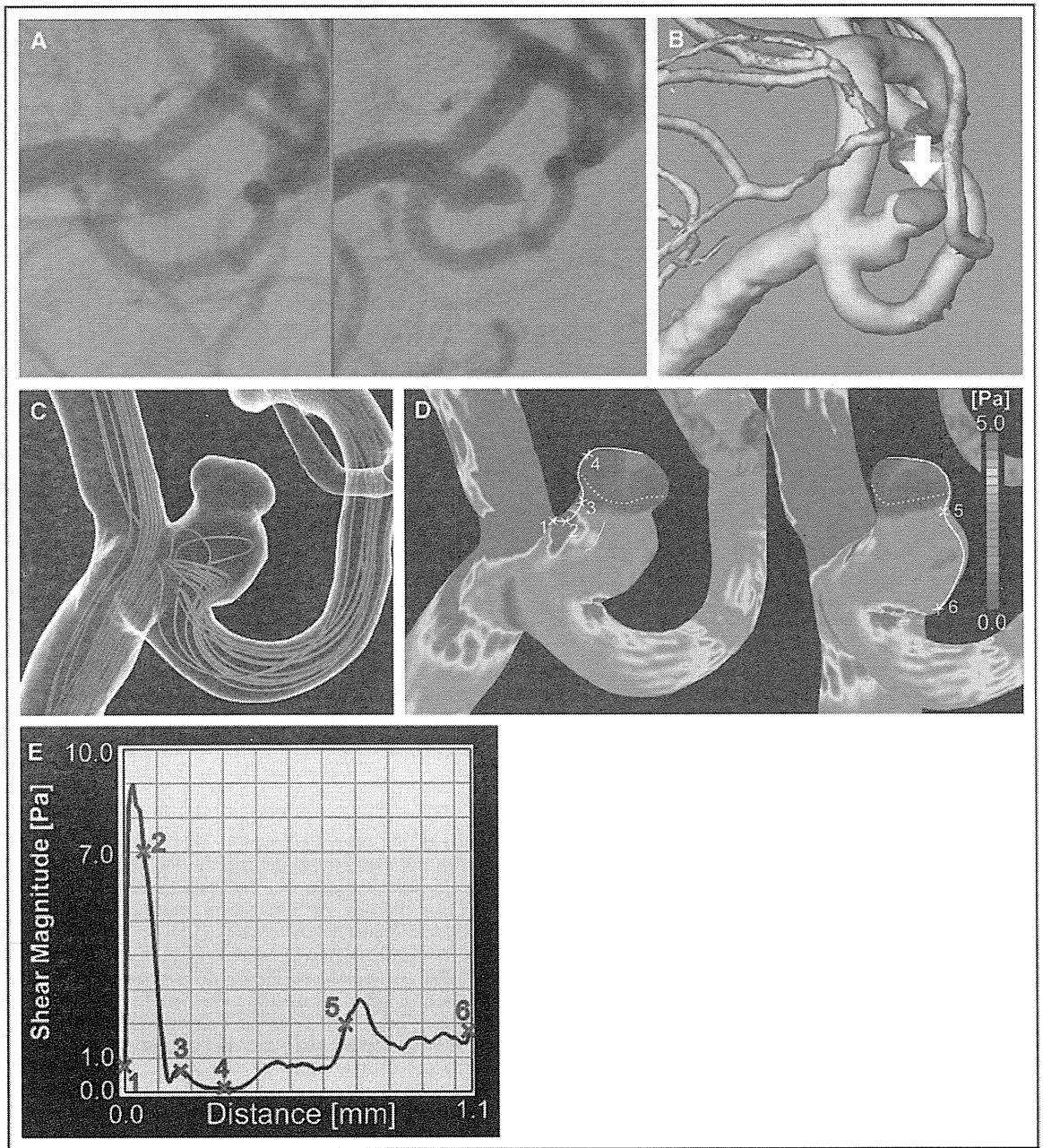

FIGURE 2. *Case 1: Left MCA aneurysm (enlarged).* **A**, *angiographic images focusing on the left MCA aneurysm before (right) and after (left) blister formation.* **B**, *coregistrated 3D surfaces of the aneurysm before (yellow) and after (red) blister formation. White arrow indicates the location of blister formation.* **C**, *Streamline visualization of intra-aneurysmal flow.* **D**, *colored contour of shear magnitude distributions. Dotted white line indicates the area of blister formation.* **E**, *plot of the shear magnitude along the white line in* **C**. *The numbers marking location on the white line in* **C** *correspond to those in* **E**. *Yellow band indicates the physiological level of shear magnitude. MCA, middle cerebral artery.*

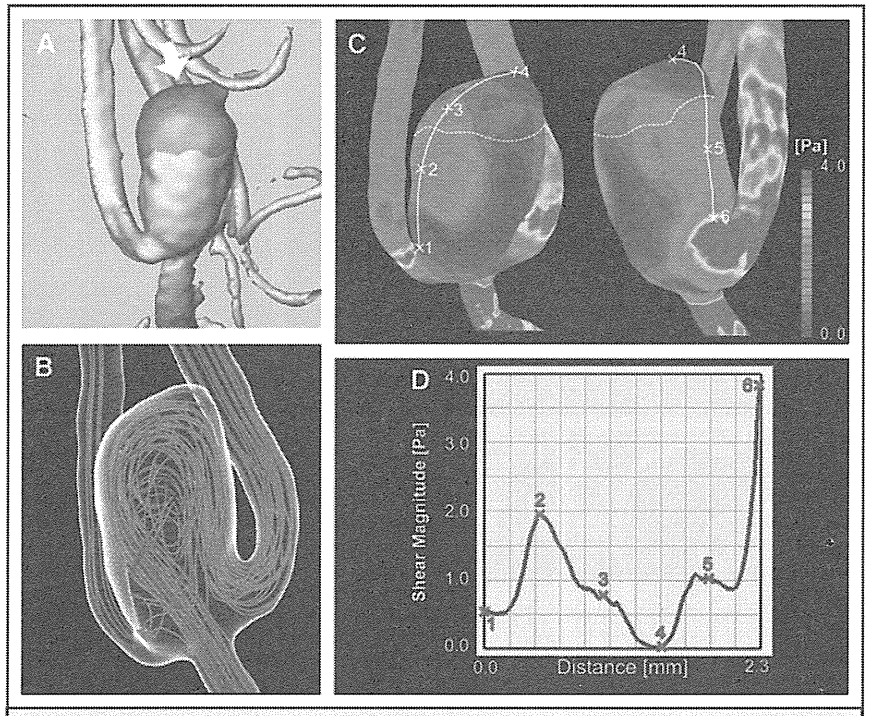

FIGURE 3. *Case 2: AComA aneurysm (ruptured).* **A,** *coregistrated 3D surfaces of the aneurysm before (yellow) and after (red) blister formation. White arrow indicates the location of blister formation.* **B,** *streamline visualization of intra-aneurysmal flow.* **C,** *colored contour of shear magnitude distributions. Dotted white line indicates the area of blister formation.* **D,** *plot of the shear magnitude along the white line in* **C**. *The numbers marking location on the white line in* **C** *correspond to those in* **D**. *Yellow band indicates the physiological level of shear magnitude. AcomA, anterior communicating artery.*

can lead to aneurysm formation,[2,11] and low shear magnitude at focally dilated segments can trigger degeneration of the vessel wall by promoting macrophage-related chronic inflammation and atherosclerotic remodeling.[9,10,12] Aoki et al[4] found that the macrophage-mediated chronic inflammation played an essential role in the progression of cerebral aneurysms in mice. Frosen et al[13] compared the pathology of the surgically resected aneurysm wall between the ruptured and unruptured cases and found that atherosclerotic changes, such as intimal hyperplasia and proliferation of disorganized smooth muscle cells, were seen more frequently in the wall of ruptured cases. These findings, in conjunction with our findings that the shear magnitude of the aneurysm wall was subphysiological and that of the blister-forming area was extremely low, imply that the progression and the rupture of the cerebral aneurysms are associated with low shear magnitude.

The present study demonstrated that the shear magnitude dropped precipitately to subphysiological levels (<1 Pa) near the border of the area of subsequent blister formation, resulting in high shear gradient at the edge of the blister-forming area. Previous reports suggest that high shear gradient has the same biological effect on the endothelium compared with low shear magnitude,[10] although endothelial cells may be more sensitive to high shear gradients than to low shear magnitude.[10] This provides a mechanistic explanation for the development of blisters at a specific area within a large area of low shear magnitude on the aneurysm wall. Cebral et al[14] indicated that small and concentrated flow impact might be an indicator of rupture-prone aneurysm; such flow impact would produce a high shear gradient near the flow impact zone and thereby accelerate the low shear-mediated degenerative process on the aneurysm wall.

Blister formation results from local weakness of the aneurysm wall and is strongly related to aneurysm rupture.[15] Blister formation is often used as an indicator of the culprit bleeding lesion when multiple aneurysms are present.[16] In 2 of the 3 present cases, rupture events coincided with blister formation. In these